Nephrol Dial Transplant (2006) 21: 869–880
doi:10.1093/ndt/gfk029
Advance Access publication 12 January 2006

Original Article

NDT
Nephrology Dialysis Transplantation

A hypothesis linking sodium and lithium reabsorption in the distal nephron

Klaus Thomsen[1] and David G. Shirley[2]

[1]Centre for Basic Psychiatric Research, Aarhus University Hospital, DK-8240 Risskov, Denmark and
[2]Centre for Nephrology, Royal Free & University College Medical School, London, UK

Abstract

Background. A hypothesis is proposed linking Na^+ and Li^+ reabsorption in the distal nephron. The handling of these two ions in the distal nephron is related because they share the same apical membrane entry mechanism: the amiloride-sensitive Na^+ channel (ENaC). However, the two ions exit the cell through different transport mechanisms: Na^+ via the Na^+-K^+-ATPase and Li^+ via the Na^+/H^+ exchanger. Studies in rats have shown that under normal circumstances hardly any Li^+ is reabsorbed in the distal nephron, so that the urinary excretion of Li^+, expressed as a fraction of the delivery to the early distal tubule ($FE_{Li\ dist}$), amounts to approximately 0.97. In contrast, during severe dietary Na^+ restriction, $FE_{Li\ dist}$ decreases to 0.50–0.60. Our hypothesis is that the absence of distal Li^+ reabsorption during intake of a normal diet can be explained by a negative driving force for Li^+ entrance across the apical membrane in those segments in which ENaC is active.

Method. We propose a model that incorporates this concept.

Results. The model indicates that the lowering of $FE_{Li\ dist}$ during dietary Na^+ restriction can be explained by activation of apical ENaC in extra sub-segments further downstream. In these extra sub-segments the driving force for Li^+ reabsorption is positive, leading to significant Li^+ reabsorption. During dietary K^+ restriction, $FE_{Li\ dist}$ is reduced to 0.35–0.55. The model shows that this reduction in $FE_{Li\ dist}$ can be explained by hyperpolarization of the apical membrane in ENaC-containing sub-segments, which is known to occur in this condition.

Conclusion. We conclude that the model may improve current understanding of both Na^+ and Li^+ handling in the distal nephron.

Correspondence and offprint requests to: Klaus Thomsen, Dr.med.sci. Centre for Basic Psychiatric Research, Aarhus University Hospital, Skovagervej 2, DK-8240 Risskov, Denmark. Email: klt@psykiatri.aaa.dk

Keywords: amiloride; collecting duct; distal nephron; epithelial sodium channel, ENaC; lithium reabsorption; sodium reabsorption

Introduction

Under normal circumstances, filtered Li^+ ions are reabsorbed in the proximal tubule (and to some extent in the loop of Henle), but virtually no Li^+ is reabsorbed in the distal nephron. This is the basis for the use of Li^+ clearance as an index of proximal tubular fluid output [1]. Surprisingly, however, when rats are given a diet that is low in either Na^+ or K^+, substantial Li^+ reabsorption does take place in the distal nephron [2–9]. The present article will address this remarkable lability of distal Li^+ transport, in an attempt not only to understand Li^+ handling itself but also to gain insight into the underlying changes in Na^+ reabsorption in the distal nephron. Because Li^+ does not have a specific transporter of its own, it must rely on other transport systems. It is our hypothesis that if current knowledge about distal nephron Na^+ reabsorption is adequate, it should be possible to calculate values for Li^+ reabsorption that match the experimentally obtained data. Conversely, if the calculated values do not concur with the experimentally obtained data, it might lead to a reassessment of our perceptions of distal nephron Na^+ handling.

First, we review those transport mechanisms that could in theory be responsible for Li^+ fluxes in distal nephron segments. Then we examine how these transport mechanisms could be stimulated by a low Na^+ diet or a low K^+ diet. Finally, we present a quantitative mapping of distal nephron Na^+ reabsorption in rats on a normal diet and in rats on a low Na^+ or low K^+ diet. We do the same for distal nephron Li^+ reabsorption under these conditions, and present a model that links the reabsorption of the two ions.

Possible transport mechanisms for Li^+ in the distal nephron

Apical membrane

Li^+ reabsorption in the distal nephron (when it occurs) must use either the paracellular route or one or more of the many transport systems located in the apical membrane. A key finding is that Li^+ reabsorption in the distal nephron is blocked by amiloride [2–8], which inhibits the conductive epithelial Na^+ channel (ENaC) present in the apical membrane. Therefore, it is highly likely that Li^+ reabsorption in the distal nephron uses this transporter rather than any of the others. Amiloride sensitivity also argues against the possibility of paracellular transport. (It should be noted that an amiloride-sensitive, non-selective cation channel has been reported in the apical membrane of cultured inner medullary collecting duct cells, but its role, if any, in Na^+ homeostasis remains undefined [10].)

The conductive epithelial Na^+ channel (ENaC). ENaC is found in tight epithelia from frog skin, toad urinary bladder, turtle colon and mammalian colon and kidney. In the mammalian nephron it has been found in the second segment of the distal convoluted tubule (DCT_2), the connecting tubule (CNT) and principal cells of the cortical collecting duct, the outer medullary collecting duct and the initial segment of the inner medullary collecting duct [10,11]. It is characterized not only by its sensitivity to amiloride but also by its low conductance, its high selectivity for Li^+ and Na^+, and its slow kinetics [12]. The ion selectivity of the channel differs among species and organs, but Li^+ traverses the channel slightly more easily than Na^+ in the rat cortical collecting duct [12].

It is known that shuttling of ENaC occurs between the cell interior and the apical membrane. Thus, the activity of apical ENaC is dictated by the balance between insertion of channels into the membrane and their retrieval into the cell interior. Recent evidence indicates that this shuttling is controlled by a complex series of regulators, of which two proteins are prominent: 'Nedd 4–2', which binds to ENaC and leads to internalization of the channel, and 'Sgk-1', which interferes with the ENaC-Nedd 4-2 interaction and thereby increases the number of channels in the apical membrane [13].

Basolateral membrane

Since any reabsorption of Li^+ occurs via ENaC, Li^+ extrusion across the basolateral membrane could only occur in DCT_2 cells, CNT cells and/or principal cells in the collecting ducts (CD). The basolateral membranes of these cells contain a large number of ion transport systems, e.g. K^+ channels, Cl^- channels, Ca^{2+}-ATPase, Na^+/Ca^{2+} exchangers, but only two could in theory transport Li^+ out of the cell: the Na^+-K^+-ATPase and the Na^+/H^+ exchanger.

The basolateral Na^+-K^+-ATPase. Li^+ is unable to substitute for Na^+ on Na^+-K^+-ATPase in frog skin or turtle colon (both, like distal nephron, 'tight' epithelia) or in human erythrocytes [14]. On the basis of these findings in non-renal systems, it seems unlikely that Na^+-K^+-ATPase could sustain significant transepithelial Li^+ transport.

The basolateral Na^+/H^+ exchanger. The Na^+/H^+ exchanger is an ubiquitous transport system. A number of isoforms (NHE 1–9) have been identified in mammalian cell membranes; the main isoform found in the basolateral membrane of the distal nephron is NHE1. The stoichiometry of the Na^+/H^+ exchanger is 1:1 and it is therefore electrically silent. The substrate selectivity of the exchanger is limited to a small number of monovalent cations, namely Na^+, H^+, Li^+ and NH_4^+. In its normally functioning mode, external Na^+ is exchanged for internal H^+. However, internal Na^+ can also be exchanged for external H^+, and internal Li^+ for external Na^+. The apparent selectivity sequence for the binding of cations to the external and internal transport sites is $H^+ \gg Li^+ > NH_4^+ > Na^+$. There is good evidence that this exchanger is responsible for basolateral membrane transport of Li^+ in amphibian tight epithelia [14], and in our view it also provides the most likely route of basolateral Li^+ transport in the mammalian distal nephron.

Stimulation of Li^+ transport in the distal nephron

Apical membrane

As indicated above, amiloride-sensitive Li^+ transport occurs through ENaC. These channels are activated by Na^+ depletion and/or chronic aldosterone stimulation [15]. However, even in Na^+-replete animals with low levels of aldosterone, some channels are active, as suggested by the substantial amiloride-induced increase in Na^+ excretion observed in rats on a normal Na^+ diet [2,3,5,9,16]. The reason why these channels do not normally reabsorb Li^+ is not immediately apparent; any model of distal Li^+ reabsorption must be constructed in a way that provides an explanation for the virtual absence of Li^+ transport during intake of a normal diet.

During administration of a low Na^+ diet, stimulation of distal nephron Li^+ reabsorption could in theory be due to increased ENaC activity, either in the sub-segments where ENaC is already present or in extra sub-segments further downstream. In a subsequent section we construct a model that allows a quantitative evaluation of these possibilities.

As discussed below, during administration of a low K^+ diet there is an increase in the potential difference across the apical membrane (PD_a) in the distal nephron. This will increase the driving force for Li^+ across the apical membrane, which could in theory lead to Li^+ transport into the cell and an increase in the intracellular Li^+ concentration, thus favouring Li^+

transport out of the cell across the basolateral membrane. Our model will also allow this possibility to be examined.

Basolateral membrane

It could be speculated that hormonal changes associated with the administration of a low Na^+ or low K^+ diet might stimulate basolateral membrane Li^+ transport and thereby support, or even drive, the changes that take place in the apical membrane. However, the evidence for this is not convincing. Increases in angiotensin II levels have been shown to have little effect on the Na^+/H^+ exchanger in the distal nephron, and we have found no evidence that aldosterone stimulates basolateral Na^+/H^+ activity in principal cells. Furthermore, direct measurements in the rat cortical collecting duct showed no activation of basolateral Na^+/H^+ exchange in rats given a low Na^+ diet for 48 h, although the apical membrane Na^+ channels were activated [15]. Thus, it is unlikely that aldosterone has a direct role in the stimulation of basolateral Li^+ transport in the distal nephron during Na^+ depletion, and it clearly has no such role during K^+ depletion since aldosterone secretion is inhibited in the latter situation.

It is concluded that a primary (as opposed to a secondary) increase in basolateral Na^+/Li^+ exchange is not the mechanism underlying stimulation of distal nephron Li^+ reabsorption in Na^+ and K^+ restriction. Accordingly, we believe that changes at the apical membrane are responsible for the observed alterations in Li^+ reabsorption.

Construction of a model of the relationship between Li^+ and Na^+ reabsorption in the distal nephron

Clearance studies using amiloride to block distal nephron Li^+ reabsorption, as well as direct micropuncture measurements, have demonstrated that in rats given a normal diet the renal Li^+ excretion, expressed as a fraction of the delivery to the early distal tubule, ($FE_{Li\ dist}$) is 0.94–1.00 (Table 1). In rats given a low Na^+ diet, $FE_{Li\ dist}$ is reduced to 0.50–0.60; and in rats given a low K^+ diet, $FE_{Li\ dist}$ is 0.35–0.55. In the following we will construct a quantitative model of Na^+ reabsorption in the distal nephron and then examine whether these values for $FE_{Li\ dist}$ can be predicted from the model.

Table 1. $FE_{Li\ dist}$ in rats given diets with different Na^+ and K^+ contents

Diet	$FE_{Li\ dist}$	References
Normal	0.94–1.00	[1]
Low Na^+	0.50–0.60	[2–4,7]
Low K^+	0.35–0.55	[3,5,6,9]

Our model applies to the nephron segments between the early distal tubule and the end of the collecting duct. It is generally considered that in micropuncture studies the early distal puncture site is located approximately halfway along the distal convoluted tubule, close to the start of its second segment (DCT_2). The late distal puncture site is, on average, located close to the junction between the CNT and the initial collecting duct, whose epithelium is identical to that of the cortical collecting duct (CCD). Accordingly, the model comprised two main segments: the accessible distal tubule (taken to be $DCT_2 + CNT$) and the collecting ducts (CD) (= CCD + outer (OMCD) and inner (IMCD) medullary collecting duct).

Establishment of the water reabsorption profile along the distal nephron

Water reabsorption along the distal nephron increases the concentration of solutes within the lumen and changes the conditions for Li^+ reabsorption. Based on determinations of osmotic water permeability and aquaporin 2 distribution [10], water reabsorption was assumed to take place in CNT and CD but not in DCT_2. In the model, the distal nephron as a whole was arbitrarily divided into 100 sub-segments and each was allocated a row in a spreadsheet. Fifteen sub-segments were arbitrarily allocated to DCT_2; therefore water reabsorption took place only in sub-segments 16–100. The model was constructed so that each of the 85 sub-segments from 16 to 100 reabsorbed the same fraction of the load delivered to that sub-segment as its neighbours. The fractional distal water excretion ($FE_{H_2O\ dist}$) was determined from measurements of inflow to the distal nephron and of outflow from the distal nephron, and water reabsorption for the 85 sub-segments was calculated accordingly.

Figure 1 illustrates the sub-division of the nephron into DCT_2, CNT and CD (CCD, OMCD and IMCD) and it indicates where information about the tubular flow is known: the early distal puncture site, the late distal puncture site and the urine. It also shows the delivery of water ($FD_{H_2O\ dist}$) along the length of the distal nephron, expressed as a fraction of delivery to the early distal tubule. Fractional delivery of water to the early distal tubule has been found by micropuncture studies to be around 0.2, and fractional urine excretion measured in both micropuncture and clearance studies averages 0.008, albeit with a good deal of scatter [6,9,16–18]. On this basis, $FE_{H_2O\ dist}$ was taken to be $0.008/0.2 = 0.04$ (see Figure 1).

Localization of the late distal puncture site and subdivision of CD

The sub-segment number where CNT ends and CD begins could be estimated from the fact that $FD_{H_2O\ dist}$ at the late distal puncture site has been measured to be approximately 0.42 [5,16–20]. In the spreadsheet, this value was found at sub-segment 38 and on this basis sub-segment 39 was taken as the first sub-segment

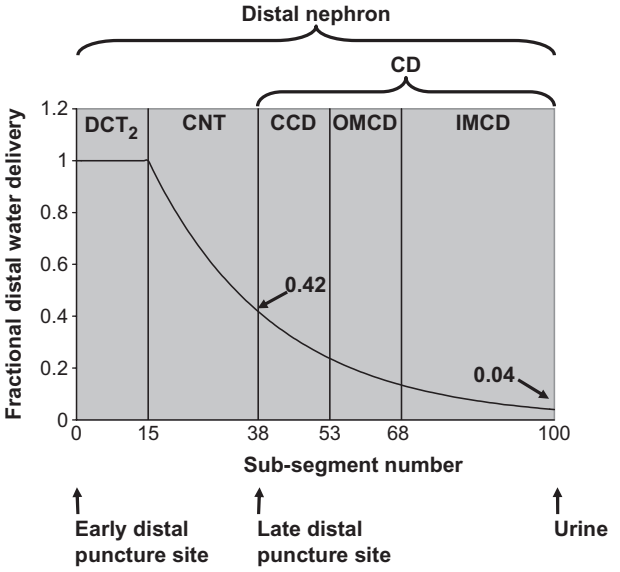

Fig. 1. Fractional water delivery to the sub-divisions of the distal nephron. The Figure illustrates the sub-division of the nephron into DCT_2, CNT and CD (CCD, OMCD and IMCD) and indicates by arrows where information about the tubular flow is known: the early distal puncture site, the late distal puncture site and the urine. The tubular flow along the length of the distal nephron ($FD_{H_2O\ dist}$) is expressed as a fraction of the delivery to the early distal tubule. It is assumed to be 1.0 throughout DCT_2 and has been measured as 0.42 at the end of CNT and 0.04 in the urine. The distal nephron is divided into 100 sub-segments that are each given a row in a spreadsheet. The sub-segment number where CNT ends and CD begins can be estimated from FD_{H_2O} measured at the late distal puncture site. In the spreadsheet, this value is found at sub-segment 38 and on this basis sub-segment 38 is taken as the last sub-segment of the CNT epithelium. Taking this into account, the sub-segments are allocated in the following way: DCT_2 1–15, CNT 16–38, CCD 39–53, OMCD 54–68 and IMCD 69–100.

of CD epithelium (Figure 1). The CD (incorporating the initial collecting duct) was arbitrarily divided into three sections: CCD, OMCD and IMCD. The relative distribution of sub-segments between these sections was approximately 1:1:2, similar to the distribution used by Weinstein [21]. In practice, CCD and OMCD were each allocated 15 sub-segments and IMCD was allocated the remaining 32 sub-segments. To summarize, the allocation of sub-segments in the present model was as follows: DCT_2, 1–15; CNT, 16–38; CCD, 39–53; OMCD, 54–68; and IMCD, 69–100.

ENaC-based and non ENaC-based Na^+ reabsorption along the nephron

In order to build the model, we used data from *in vivo* clearance and micropuncture studies. We determined, from the literature, the fractional distal delivery of Na^+ ($FD_{Na\ dist}$) to the end of CNT and the fractional distal Na^+ excretion ($FE_{Na\ dist}$). The relative contributions of ENaC-mediated and non-ENaC-mediated Na^+ reabsorption were calculated on the basis of studies that have used amiloride to block ENaC-mediated Na^+ reabsorption. $FE_{Na\ dist}$ with or without amiloride was calculated as the fractional Na^+ excretion (FE_{Na}) divided by the fractional Na^+ delivery to the early distal tubule. The latter was taken from micropuncture studies to be 0.08 in rats on a normal diet and 0.06 in rats on a low Na^+ diet or a low K^+ diet [4,5,8,16,22]. $FE_{Na\ dist}$ for each individual study is shown in Table 2, and average values for each of the three diets are indicated.

Table 2. $FE_{Na\ dist}$ with and without blockade of ENaC with amiloride

Authors	$FE_{Na\ dist}$ without blockade of ENaC	$FE_{Na\ dist}$ with blockade of ENaC
Normal diet		
Duarte *et al.* [32]	0.231	0.370
Shirley *et al.* [16]	0.038	0.467
Fransen *et al.* [8]	0.017	0.247
Thomsen *et al.* [3]	0.084	0.273
Thomsen and Shalmi [6]	0.108	0.194
Shalmi *et al.* [2]	0.066	0.326
Thomsen *et al.* [33]	0.075	0.431
Emamifar *et al.* [9]	0.103	0.268
Thomsen *et al.* [34]	0.034	0.171
Average	**0.084**	**0.305**
Low Na^+ diet		
Kirchner [7]	0.0050	0.155
Thomsen *et al.* [3]	0.0046	0.328
Walter *et al.* [4]	0.0051	0.222
Shalmi *et al.* [2]	0.0080	0.287
Average	**0.0057**	**0.248**
Low K^+ diet		
Thomsen *et al.* [3]	0.077	0.241
Shirley and Walter [5]	0.077	0.246
Thomsen and Shalmi [6]	0.120	0.244
Emamifar *et al.* [9]	0.142	0.502
Average	**0.104**	**0.308**

Similarly, $FD_{Na\ dist}$ to the end of CNT with or without amiloride was calculated. For this variable, there were no obvious differences between diets; therefore, the data were pooled. $FD_{Na\ dist}$ at the end of CNT averaged 0.40 [4,5,16–20,23] and this value rose by 0.08 when ENaC was blocked by amiloride [4,5,16].

Na^+ reabsorption in each sub-segment was expressed as a fraction of the load delivered to that sub-segment. For ENaC-based Na^+ reabsorption, this fraction was designated A1 in $DCT_2 + CNT$ and A2 in CD. For non-ENaC-based mechanisms, the corresponding values were designated B1 and B2. On the basis of known ENaC distribution in the distal tubule [10], it was assumed that ENaC-based Na^+ reabsorption increases gradually from the beginning of DCT_2 to the end of CNT and, therefore, A1 was multiplied by a factor that increased linearly from zero to unity.

The first step was to find the appropriate values for B1 and B2. It was assumed that during amiloride administration both A1 and A2 were zero; B1 and B2 were then given appropriate values so that $FD_{Na\ dist}$ at the end of CNT and $FE_{Na\ dist}$ became equal to the values found in practice under these conditions (Table 3). Subsequently, the values for A1 and A2 under normal circumstances were given appropriate values so that $FD_{Na\ dist}$ at the end of CNT and $FE_{Na\ dist}$

Table 3. Na^+ reabsorption in each sub-segment expressed as a fraction of the load delivered to that sub-segment. For ENaC-based Na^+ reabsorption, this fraction was designated A1 in $DCT_2 + CNT$ and A2 in CD; for extra sub-segments inserted in rats on a low Na^+ diet, the fraction was designated A3. For non-ENaC-based mechanisms, the corresponding values were designated B1 and B2

	A1	A2	A3	B1	B2
Normal diet	0.00910	0.1041		0.01913	0.00729
Low Na^+ diet	0.00910	0.1041	0.058	0.01913	0.01060
Low K^+ diet	0.00910	0.0858		0.01913	0.00713

became equal to the values found in practice when no amiloride was administered.

It should be noted that, in our model, ENaC-mediated Na^+ reabsorption in the CCD exceeded that in $DCT_2 + CNT$, which contrasts with a recent suggestion that ENaC-mediated Na^+ reabsorption in the distal tubule is higher than that in CCD [13]. The latter view is supported by *in vitro* studies indicating a higher rate of basal Na^+ transport in isolated perfused segments of rabbit CNT *vs* CCD and higher amiloride-sensitive currents in cell-attached patches in CNT *vs* CCD from rats previously infused with aldosterone. Moreover, in rabbit and mouse at least, there appears to be an axial gradient of alpha-ENaC sub-unit expression at the apical membrane, with greatest expression in CNT and least in MCD [13]. However, whilst acknowledging the strength of these *in vitro* and molecular data, it must be emphasized that our model is based on *in vivo* measurements in the rat, where ENaC-mediated reabsorption has been inhibited pharmacologically. It is only in these *in vivo* situations that corresponding data for Li^+ reabsorption are available.

Calculation of the driving force for Li^+ reabsorption along the distal nephron

The transport of Li^+ across the apical membrane depends on the driving force, which can be expressed as $PD_a - E_{Li}$, where PD_a is the potential difference across the apical membrane and E_{Li} is the equilibrium potential for Li^+ across the apical membrane. E_{Li} can be calculated using the Nernst equation. At 37°C,

$$E_{Li} = 26.8 \times \ln([Li^+]_{cell}/[Li^+]_{TF}),$$

where, $[Li^+]_{cell}$ and $[Li^+]_{TF}$ are the concentrations of Li^+ in the cell and tubular fluid, respectively. Therefore, the driving force can be calculated as:

$$\text{Driving force} = PD_a - 26.8 \times \ln([Li^+]_{cell}/[Li^+]_{TF}) \quad (1)$$

Since $[Li^+]_{cell}$ and $[Li^+]_{TF}$ vary with the amount of Li^+ given as a test dose, whereas the same values divided by the plasma Li^+ concentration ($[Li^+]_{cell/P}$ and $[Li^+]_{TF/P}$, respectively) do not, the latter values were used in our calculations.

$[Li^+]_{TF/P}$ has been measured as 1.3 at the early distal puncture site [16]. This was therefore used as the starting value ($[Li^+]_{TF/P\ initial}$) in the spreadsheet. $[Li^+]_{TF/P}$ values for subsequent sub-segments were calculated taking into account water reabsorption and Li^+ reabsorption, if any, in the preceding sub-segments.

On the basis of measurements of transepithelial PD, together in some cases with measurement of basolateral PD [24], PD_a in our model fell steadily from 85 mV at the beginning of DCT_2 to 45 mV at the beginning of CD. In CD, PD_a was taken to be 45 mV in those sub-segments with active ENaC and 85 mV in the remaining sub-segments.

Localization of ENaC-mediated and non-ENaC-mediated Na^+ transport

As already indicated, although the exact reabsorption profile along the distal tubule is unknown, in the model we inserted ENaC into the apical membrane of all sub-segments in $DCT_2 + CNT$, with gradually increasing activity towards CCD. This may or may not be correct, but in practice the exact reabsorption profile in these segments has negligible impact on the outcome of the model because Li^+ reabsorption here, when present at all, is very low due to a low driving force for Li^+.

The more critical step was to determine the number of sub-segments involved in ENaC-mediated Na^+ reabsorption beyond the CNT. During intake of a normal diet, some studies find that Li^+ reabsorption in the distal nephron is completely absent [1]; it is evident that in this case the final sub-segment with active ENaC cannot be located where the driving force for Li^+ is positive. In other studies [1], Li^+ reabsorption is small but finite (2–6% of the load delivered to the early distal tubule); here, the final sub-segment with active ENaC must be located somewhere downstream of the point where the driving force for Li^+ has become positive. Taking a consensus, we have constructed the model so that $FE_{Li\ dist}$ has a value of 0.97 in rats on a normal diet (Table 1).

As indicated in equation 1, the value for $[Li^+]_{cell/P}$ influences the driving force for Li^+ across the apical membrane and thereby the precise location of the sub-segment where the driving force for Li^+ reabsorption changes from negative to positive. The higher the $[Li^+]_{cell/P}$, the greater the number of sub-segments with a negative driving force for Li^+, i.e. the more distally Li^+ reabsorption starts. No measurements of $[Li^+]_{cell/P}$ are available for the collecting duct, so it was necessary to make an assumption. We elected to use a $[Li^+]_{cell/P}$ value of 21. In this case, ENaC would need to be activated in two-thirds of the 15 sub-segments of CCD to provide a value for $FE_{Li\ dist}$ of 0.97. Although it is acknowledged that we cannot know the precise location of the final ENaC-containing sub-segment, this assumption accords with the general belief that on a normal diet ENaC is active in most of CCD. A value for $[Li^+]_{cell/P}$ of 21 is also consistent with direct measurements in non-renal tissues [25].

In these calculations, we took into account the cortico-papillary Li^+ concentration gradient. It has been shown that the Li^+ concentration in papillary interstitial fluid (in the rat) is approximately 3 times higher than that of systemic plasma [26]. For the model,

it was considered that when the extracellular Li^+ concentration rose by a factor of 3 from cortex to papilla, the intracellular Li^+ concentration would increase by the same factor. We therefore introduced into the spreadsheet a gradient from 1 to 3, starting at the end of CCD and ending in the last sub-segment of IMCD. $[Li^+]_{cell/P}$ was multiplied by this gradient.

When a low Na^+ diet or a low K^+ diet stimulates Li^+ reabsorption, this will inevitably lead to an increase in $[Li^+]_{cell/P}$. It is impossible to predict whether this increase will be trivial or significant; it will depend on the capacity of the basolateral Na^+/Li^+ exchange mechanism. Any increase in $[Li^+]_{cell/P}$ will tend to reduce Li^+ reabsorption, and in the model it may therefore be necessary to make minor adjustments to the activation of ENaC or to PD_a during dietary Na^+ or K^+ restriction in order to obtain the required $FE_{Li\ dist}$. However, this will not influence the overall conclusions drawn from our presentation.

It was difficult to determine where non-ENaC-based Na^+ reabsorption should be located. Combined *in situ* hybridization and immunohistochemistry studies have shown that Na^+Cl^- co-transporter (NCC) expression begins abruptly at the transition from the thick ascending limb to the DCT and ends at the transition from DCT to CNT [27]. However, other studies have suggested that significant thiazide-sensitive Na^+ reabsorption takes place beyond the late distal puncture site, and amiloride-insensitive Na^+ transport has been demonstrated as far as IMCD [28]. In the model, we allocated the non-ENaC-mediated Na^+ reabsorption evenly along $DCT_2 + CNT$ and evenly along CD.

Calculation of Li^+ reabsorption in relation to Na^+ reabsorption

If two ions are reabsorbed through the same channel, and if the permeability and driving force for the two ions are the same, as for ^{22}Na and ^{23}Na for example, the reabsorbed fraction of the two ions will be the same. If, on the other hand, the driving forces for the two ions are different, as for Na^+ and Li^+, the ratio between the reabsorbed fractions of the two ions in a particular sub-segment can be calculated on the basis of the ratio between fluxes for the two ions, using the Goldman-Hodgkin-Katz equation [29].

Li^+ reabsorption in a particular sub-segment, expressed as a fraction of Li^+ delivery to that sub-segment, can be expressed as:

$$R_{Li} = J_{Li} \times Area/([Li^+]_{TF} \times V_{TF}),$$

where J_{Li} is the net Li^+ flux, Area is the surface area of the sub-segment and V_{TF} is the tubular flow rate to that sub-segment. Similarly, the ENaC-based reabsorbed fraction of Na^+ (R_{Na}) in a particular sub-segment is

$$R_{Na} = J_{Na} \times Area/([Na^+]_{TF} \times V_{TF}).$$

It follows that

$$R_{Li}/R_{Na} = (J_{Li}/J_{Na}) \times ([Na^+]_{TF}/[Li^+]_{TF}) \quad (2)$$

At 37°C, the Li^+ flux is calculated by the Goldman-Hodgkin-Katz equation as

$$J_{Li} = -P_{Li} \times (-PD_a \times 0.0375) \times [[Li^+]_{TF} - [Li^+]_{cell} \times \exp(-PD_a \times 0.0375)]/[1 - \exp(-PD_a \times 0.0375)] \quad (3)$$

Similarly, the Na^+ flux is calculated as

$$J_{Na} = -P_{Na} \times (-PD_a \times 0.0375) \times [[Na^+]_{TF} - [Na^+]_{cell} \times \exp(-PD_a \times 0.0375)]/[1 - \exp(-PD_a \times 0.0375)] \quad (4)$$

where, P_{Li} and P_{Na} are the permeabilities to Li^+ and Na^+, respectively.

By insertion of equations 3 and 4 in equation 2 we come to the following:

$$R_{Li}/R_{Na} = (P_{Li}/P_{Na}) \times ([Na^+]_{TF}/[Li^+]_{TF}) \times [[Li^+]_{TF} - [Li^+]_{cell} \times \exp(-PD_a \times 0.0375)]/[[Na^+]_{TF} - [Na^+]_{cell} \times \exp(-PD_a \times 0.0375)].$$

At 37°C, the single-channel conductance for Na^+ is 7 pS and that for Li^+ is 12 pS [12]. Furthermore, $[Li^+]_{TF}$ and $[Li^+]_{cell}$ can be replaced by $[Li^+]_{TF/P}$ and $[Li^+]_{cell/P}$, for reasons explained previously, and, for the sake of uniformity, $[Na^+]_{cell/P}$ and $[Na^+]_{TF/P}$ can be introduced instead of $[Na^+]_{cell}$ and $[Na^+]_{TF}$. This leads to the following:

$$R_{Li} = R_{Na} \times (12/7) \times ([Na^+]_{TF/P}/[Li^+]_{TF/P}) \times [[Li^+]_{TF/P} - [Li^+]_{cell/P} \times \exp(-PD_a \times 0.0375)]/[[Na^+]_{TF/P} - [Na^+]_{cell/P} \times \exp(-PD_a \times 0.0375)] \quad (5)$$

This expression provides the opportunity of calculating the fractional reabsorption of Li^+ from the fractional ENaC-based Na^+ reabsorption for each sub-segment, and consequently of calculating the total Li^+ reabsorption for all ENaC-containing sub-segments in the distal nephron.

Implementation of the model

Rats on a normal diet

Table 4 summarizes the data entered into the model. For rats on a normal diet, the following values were used: $[Li^+]_{cell/P} = 21$; $[Li^+]_{TF/P\ initial} = 1.3$; $[Na^+]_{cell} = 10$ mM; $[Na^+]_{TF\ initial} = 50$ mM; $FE_{Na\ dist} = 0.084$; and $FE_{H2O\ dist} = 0.04$. As indicated above, we assumed that in rats on a normal diet ENaC is present throughout $DCT_2 + CNT$ and in sub-segments 39–48 in CD. With these premises entered into the model, values for fractional distal Na^+ reabsorption in $DCT_2 + CNT$ and in CD were as indicated in Table 5 and $FE_{Li\ dist}$

Table 4. Characteristics of the model

Diet	Normal	Low Na^+	Low K^+
$FD_{H_2O\ dist}$ in sub-segments 1–15	1.00	1.00	1.00
$FD_{H_2O\ dist}$ at the end of CNT	0.42	0.42	0.42
$FE_{H_2O\ dist}$	0.04	0.04	0.04
$[Na^+]_{cell}$ (mM)	10	10	10
$[Na^+]_{TF}$ in sub-segment 1 (mM)	50	50	50
$FD_{Na\ dist}$ in sub-segment 1	1.00	1.00	1.00
$FD_{Na\ dist}$ at the end of CNT			
without amiloride	0.40	0.40	0.40
with amiloride	0.48	0.48	0.48
$FE_{Na\ dist}$			
without amiloride	0.084	0.006	0.104
with amiloride	0.305	0.248	0.308
Sub-segments with active ENaC	1–48	1–89	1–48
$FD_{Li\ dist}$ in sub-segment 1	1.00	1.00	1.00
$[Li^+]_{cell/P}$	21	21	21
$[Li^+]_{TF/P}$ in sub-segment 1	1.3	1.2	1.8
PD_a in DCT_2 and CNT (mV)	85→45	85→45	85→65
PD_a in CD with active ENaC (mV)	45	45	65
PD_a in sub-segments without active ENaC (mV)	85	85	85

Table 5. Fractional distal Na^+ reabsorption in rats on a normal, low Na^+ or low K^+ diet

		ENaC	Non-ENaC	Total
Normal diet	DCT_2 + CNT	0.10	0.50	0.60
	CD	0.26	0.06	0.32
	Total	0.36	0.56	0.92
Low Na^+ diet	DCT_2 + CNT	0.10	0.50	0.60
	CD	0.35	0.04	0.39
	Total	0.45	0.54	0.99
Low K^+ diet	DCT_2 + CNT	0.10	0.50	0.60
	CD	0.23	0.07	0.30
	Total	0.33	0.57	0.90

was 0.97 (Figure 2), in accordance with experimentally observed values [1].

Rats on a low Na^+ diet

In rats given a low Na^+ diet, $FE_{Li\ dist}$ is reduced to 0.50–0.60 (Table 1).

In order to comply with the conditions of a low Na^+ diet, the model was modified in the following ways: $[Li^+]_{TF/P\ initial}$ was lowered slightly, to 1.2 [4], and the values for ENaC-based and non ENaC-based Na^+ reabsorption were adjusted to achieve distal deliveries of Na^+ to the end of CNT and to the urine in accordance with experimentally observed values (Table 4). To reduce Na^+ excretion in the model to match that seen in practice, we first increased ENaC activity in those sub-segments in which it was already present. However, this resulted in hardly any change in $FE_{Li\ dist}$, because the driving force for Li^+ reabsorption in those segments was insufficient. Our next strategy was to extend the number of sub-segments with active apical ENaC further downstream. Here the conditions for Li^+ reabsorption are more favourable because the continued water reabsorption leads to an increase in $[Li^+]_{TF/P}$. When ENaC was activated as far as sub-segment 89 in the model and Na^+ reabsorption per sub-segment was adjusted accordingly, values for fractional distal Na^+ reabsorption in DCT_2 + CNT and in CD were as indicated in Table 5 and $FE_{Li\ dist}$ was 0.55 (Figure 3), i.e. in the middle of the range of experimentally observed values.

Our conclusion, that administration of a low Na^+ diet is associated with insertion of ENaC into the apical membrane in extra sub-segments further downstream, is compatible with observations on alpha, beta and gamma ENaC sub-units in rat kidney [11]. Immuno-electron microscopy showed that alpha ENaC was present in a narrow zone near the apical membrane in CCD and OMCD, whereas alpha-ENaC labelling in IMCD cells was distributed throughout the cytoplasm, suggesting readiness of ENaC to be activated in this area. Our conclusion is also consistent with the view expressed by Loffing *et al.* [30] that elevated plasma aldosterone levels (induced by exogenous application or by chronically low dietary sodium intake) appear to extend the portion of the aldosterone-sensitive distal nephron in which all three sub-units are localized apically.

Rats on a low K^+ diet

In rats given a low K^+ diet, $FE_{Li\ dist}$ is reduced to 0.35–0.55 (Table 1).

Administration of a low K^+ diet leads to a reduction in the transepithelial PD in the distal tubule, suggesting that PD_a is increased [31]. It has been proposed that the Li^+ reabsorption in the distal nephron seen during K^+ depletion might be due to this hyperpolarization of the apical membrane [5]. Therefore, we examined whether the model would provide values for $FE_{Li\ dist}$ comparable to those observed in practice if PD_a was increased in all sub-segments with active ENaC. $[Li]_{TF/P\ initial}$ was given a value of 1.8, as measured in rats on a low K^+ diet [5]. Under these conditions, the model showed that values for fractional distal Na^+ reabsorption in DCT_2 + CNT and in CD were as indicated in Table 5 and that, when PD_a was increased to 65 mV, $FE_{Li\ dist}$ was 0.45 (Figure 4), i.e. in the middle of the range of experimentally observed values.

Thus, the prediction from the model supports the proposition that an increase in PD_a may be responsible for lowering $FE_{Li\ dist}$ during administration of a low K^+ diet.

Conclusions concerning distal nephron Na^+ and Li^+ handling

It is concluded that during intake of a normal diet, the majority of ENaC-based Na^+ reabsorption takes place in the first part of the collecting duct. There is

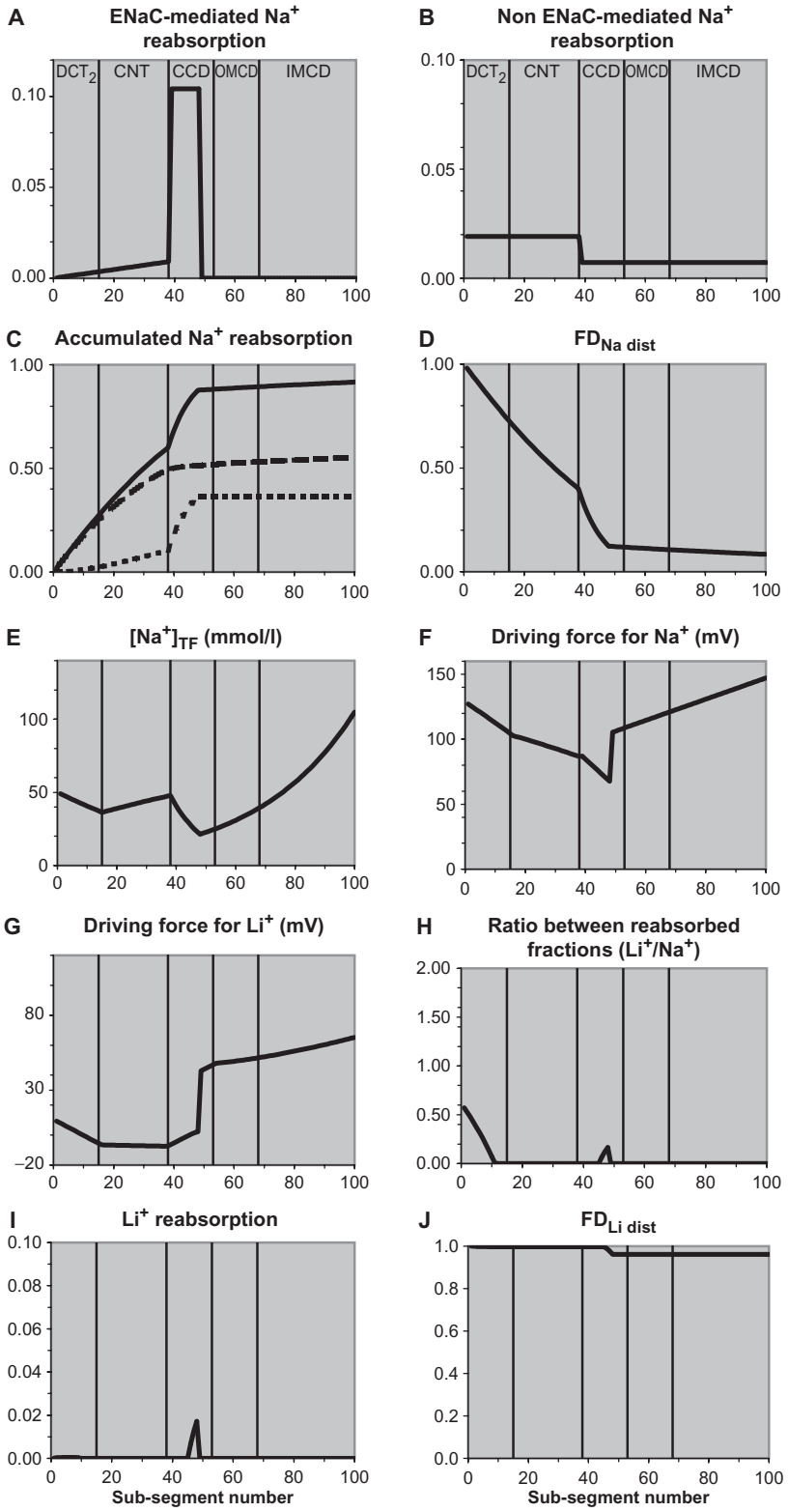

Fig. 2. Normal diet. The Figure shows Na^+ reabsorption for each sub-segment by (**A**) ENaC-based and (**B**) non-ENaC-based mechanisms, expressed as fractions of Na^+ delivery to each sub-segment; (**C**) accumulated Na^+ reabsorption, expressed as a fraction of Na^+ delivery to the early distal tubule, by ENaC (···), non-ENaC (- - -) and total (—); (**D**) Na^+ delivery ($FD_{Na\ dist}$), expressed as a fraction of the delivery to the early distal tubule; (**E**) $[Na^+]_{TF}$; (**F** and **G**) the driving forces for Na^+ and Li^+; (**H**) the ratio between Li^+ reabsorption and ENaC-mediated Na^+ reabsorption for each sub-segment, expressed as fractions of delivery to each sub-segment; (**I**) Li^+ reabsorption for each sub-segment, expressed as a fraction of Li^+ delivery to each sub-segment; (**J**) Li^+ delivery ($FD_{Li\ dist}$), expressed as a fraction of the delivery to the early distal tubule. The sub-segments in CCD are the ones with significant ENaC activity in rats given a normal diet and the only ones where significant Li^+ reabsorption can potentially take place, but the Li^+ reabsorption is trivial because the driving force for Li^+ is negative in most of the CCD.

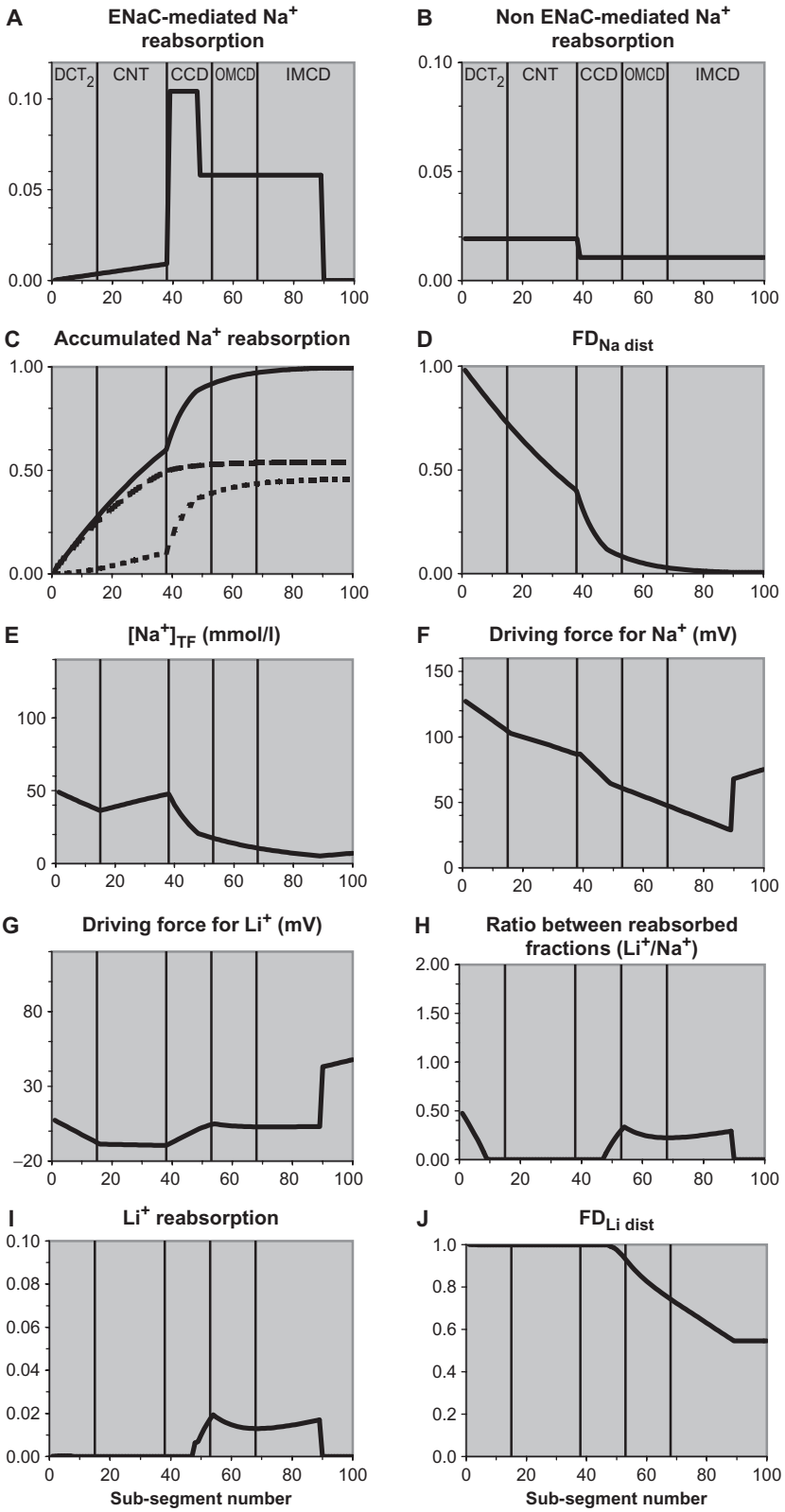

Fig. 3. Low Na^+ diet. In order to reduce $FE_{Na\ dist}$ and $FE_{Li\ dist}$ appropriately, ENaC is activated in the apical membrane in sub-segments further downstream where the conditions for Li^+ reabsorption are more favourable due to a higher degree of water reabsorption. The exact reabsorption profile is unknown but the figure shows an example.

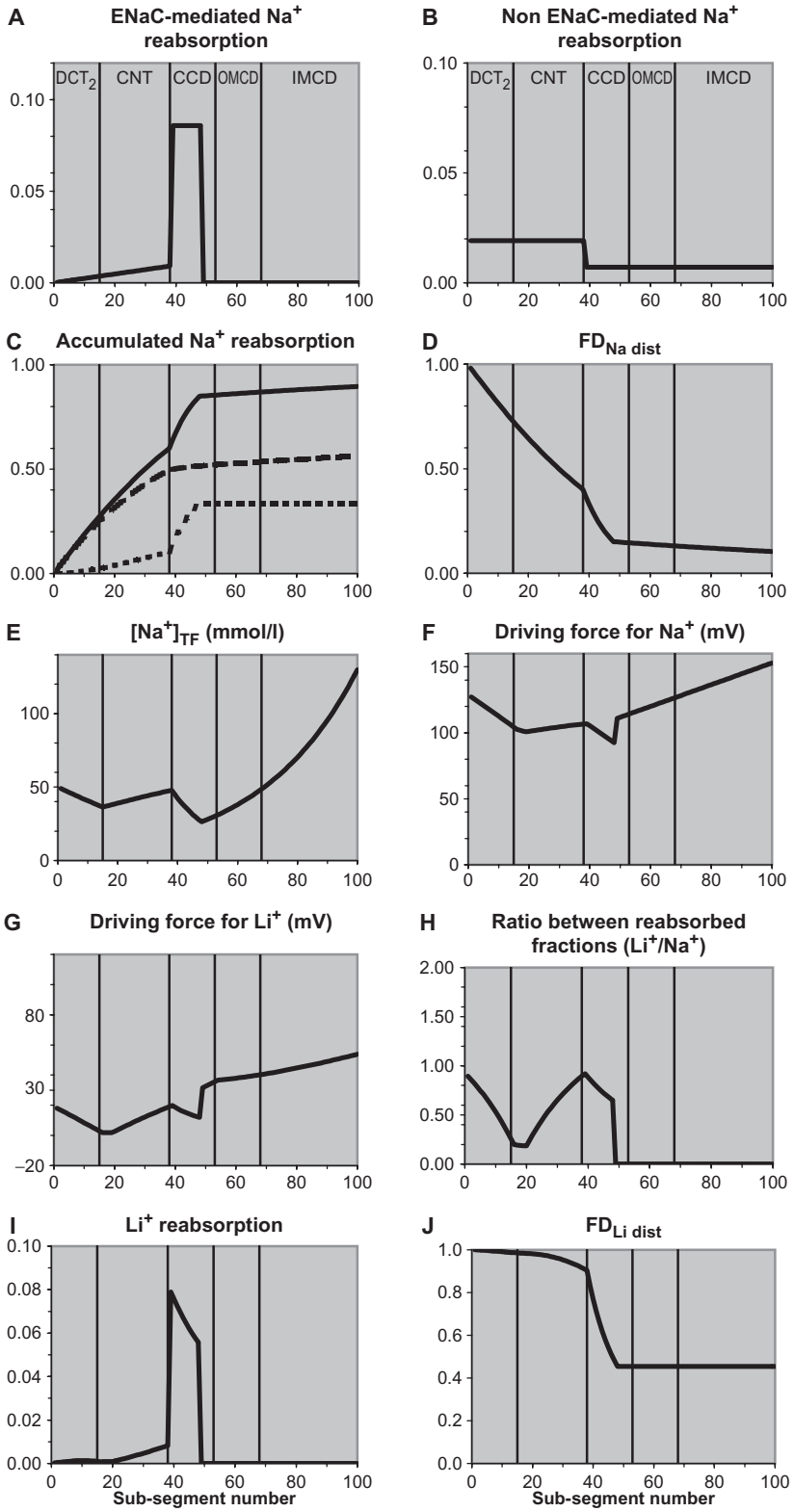

Fig. 4. Low K^+ diet. In low K^+ rats, $[Li^+]_{TF/P\ initial}$ is 1.8 and PD_a is increased from 45 to 65 mV. The driving force for Li^+ is therefore increased, leading to Li^+ reabsorption in all sub-segments with active ENaC.

virtually no Li^+ reabsorption, because the driving force for Li^+ reabsorption is negative in most of these tubular segments. During intake of a low Na^+ diet, urinary Na^+ excretion decreases to extremely low values. Such values cannot be attained simply by increased activity of ENaC channels in existing segments because this would not lead to the significant increase in distal nephron Li^+ reabsorption observed in practice. The

low Na^+ excretion can only be established by insertion of ENaC into the apical membrane of additional sub-segments further downstream where the conditions for Li^+ reabsorption are more favourable due to continued water reabsorption. In these sub-segments, the driving force for Li^+ is positive and Li^+ is therefore reabsorbed. During intake of a low K^+ diet, there is a reduction in $FE_{Li\ dist}$ that can be explained by hyperpolarization of the apical membrane of ENaC-containing sub-segments.

Consequences for the use of the Li^+ clearance technique

The Li^+ clearance technique for the measurement of proximal tubular fluid output is based on the assumptions that Li^+ is reabsorbed in the proximal tubules to the same degree as Na^+ and water, and that no Li^+ is reabsorbed in the distal nephron. Clearance and micropuncture studies in rats have confirmed that the latter assumption is largely correct under normal conditions, whereas significant Li^+ reabsorption in the distal nephron occurs when rats are given a low Na^+ diet or a low K^+ diet. The difficulty in understanding the mechanisms underlying these dietary-induced changes in distal Li^+ reabsorption has fuelled some uncertainty concerning the reliability of the technique. We believe therefore that, in addition to addressing an academically interesting question, the present investigation might be useful to those who employ the technique: the model presented shows why it can be used under some circumstances but not others.

Conflict of interest statement. None declared.

References

1. Thomsen K, Shirley DG. The validity of lithium clearance as an index of sodium and water delivery from the proximal tubules. *Nephron* 1997; 77: 125–138
2. Shalmi M, Jonassen TEN, Thomsen K, Kibble JD, Bie P, Christensen S. Model explaining the relation between distal nephron Li^+ reabsorption and urinary Na^+ excretion in rats. *Am J Physiol Renal Physiol* 1998; 274: F445–F452
3. Thomsen K, Shalmi M, Olesen OV. Effect of low dietary sodium and potassium on lithium clearance in rats. *Miner Electrolyte Metab* 1993; 19: 91–98
4. Walter SJ, Sampson B, Shirley DG. A micropuncture study of renal tubular lithium reabsorption in sodium-depleted rats. *J Physiol (Lond)* 1995; 483: 473–479
5. Shirley DG, Walter SJ. Renal tubular lithium reabsorption in potassium-depleted rats. *J Physiol (Lond)* 1997; 501: 663–670
6. Thomsen K, Shalmi M. Effect of adrenalectomy on distal nephron lithium reabsorption induced by potassium depletion. *Kidney Blood Pres Re* 1997; 20: 31–37
7. Kirchner KA. Lithium as a marker for proximal tubular delivery during low salt intake and diuretic infusion. *Am J Physiol Renal Fluid Electrolyte Physiol* 1987; 253: F188–F196
8. Fransen R, Boer WH, Boer P, Koomans HA. Amiloride-sensitive lithium reabsorption in rats: a micropuncture study. *J Pharmacol Exp Ther* 1992; 263: 646–650
9. Emamifar M, Shalmi M, Thomsen K, Christensen S. Mechanisms of distal nephron Li^+ reabsorption during dietary K^+ restriction in rats. *Kidney Blood Press Res* 2000; 23: 83–88
10. Shirley DG, Unwin RJ. Structure and function of the tubules. In: Davison AM, Cameron JS, Grünfeld J-P *et al*., eds. *Oxford Textbook of Clinical Nephrology*. Oxford University Press, Oxford: 2005: 923–942
11. Hager H, Kwon TH, Vinnikova AK *et al*. Immunocytochemical and immunoelectron microscopic localization of alpha-, beta-, and gamma-ENaC in rat kidney. *Am J Physiol Renal Physiol* 2001; 280: F1093–F1106
12. Palmer LG, Garty H. Epithelial Na channels. In: Seldin DW, Giebisch G, eds. *The Kidney. Physiology and Pathophysiology*. Lippincott Williams & Wilkins, Philadelphia: 2000: 251–276
13. Meneton P, Loffing J, Warnock DG. Sodium and potassium handling by the aldosterone-sensitive distal nephron: the pivotal role of the distal and connecting tubule. *Am J Physiol Renal Physiol* 2004; 287: F593–F601
14. Holstein-Rathlou NH. Lithium transport across biological membranes. *Kidney Int* 1990; 37 [Suppl 28]: 4–9
15. Pacha J, Frindt G, Antonian L, Silver RB, Palmer LG. Regulation of Na channels of the rat cortical collecting tubule by aldosterone. *J Gen Physiol* 1993; 102: 25–42
16. Shirley DG, Walter SJ, Sampson B. A micropuncture study of renal lithium reabsorption: effects of amiloride and furosemide. *Am J Physiol Renal Fluid Electrolyte Physiol* 1992; 263: F1128–F1133
17. Hropot M, Fowler N, Karlmark B, Giebisch G. Tubular action of diuretics: distal effects on electrolyte transport and acidification. *Kidney Int* 1985; 28: 477–489
18. Walter SJ, Shore AC, Shirley DG. Effect of potassium depletion on renal tubular function in the rat. *Clin Sci* 1988; 75: 621–628
19. Shirley DG, Walter SJ. Acute and chronic changes in renal function following unilateral nephrectomy. *Kidney Int* 1991; 40: 62–68
20. Walter SJ, Shirley DG. The effect of chronic hydrochlorothiazide administration on renal function in the rat. *Clin Sci* 1986; 70: 379–387
21. Weinstein AM. A mathematical model of rat collecting duct. I. Flow effects on transport and urinary acidification. *Am J Physiol Renal Physiol* 2002; 283: F1237–F1251
22. Fransen R, Boer WH, De Roos R, Boer P, Koomans HA. Effects of low-dose angiotensin II infusion on loop segment reabsorption: a free-flow micropuncture study in rats. *Clin Sci* 1995; 88: 351–358
23. Shirley DG, Skinner J, Walter SJ. The influence of dietary potassium on the renal tubular effect of hydrochlorothiazide in the rat. *Br J Pharmacol* 1987; 91: 693–699
24. Reilly RF, Ellison DH. Mammalian distal tubule: physiology, pathophysiology, and molecular anatomy. *Physiol Rev* 2000; 80: 277–313
25. Leblanc G. The mechanism of lithium accumulation in the isolated frog skin epithelium. *Pflügers Arch* 1972; 337: 1–18
26. Taniguchi J, Shirley DG, Walter SJ, Imai M. Simulation of lithium transport along the thin segments of Henle's loop. *Kidney Int* 1993; 44: 337–343
27. Schmitt R, Ellison DH, Farman N *et al*. Developmental expression of sodium entry pathways in rat nephron. *Am J Physiol Renal Physiol* 1999; 276: F367–F381
28. Nonaka T, Matsuzaki K, Kawahara K, Suzuki K, Hoshino M. Monovalent cation selective channel in the apical membrane of rat inner medullary collecting duct cells in primary culture. *Biochim Biophys Acta* 1995; 1233: 163–174
29. Reuss L. Basic mechanisms of ion transport. In: Seldin DW, Giebisch G, eds. *The Kidney. Physiology and Pathophysiology*. Lippincott Williams & Wilkins, Philadelphia: 2000: 85–106
30. Loffing J, Summa V, Zecevic M, Verrey F. Mediators of aldosterone action in the renal tubule. *Curr Opin Nephrol Hypertens* 2001; 10: 667–675

31. Bailey M, Capasso G, Agulian S, Giebisch G, Unwin R. The relationship between distal tubular proton secretion and dietary potassium depletion: evidence for up-regulation of H^+-ATPase. *Nephrol Dial Transplant* 1999; 14: 1435–1440
32. Duarte CG, Chomety F, Giebisch G. Effect of amiloride, ouabain, and furosemide on distal tubular function in the rat. *Am J Physiol* 1971; 221: 632–640
33. Thomsen K, Bak M, Shirley DG. Chronic lithium treatment inhibits amiloride-sensitive sodium transport in the rat distal nephron. *J Pharmacol Exp Ther* 1999; 289: 443–447
34. Thomsen K, Jonassen TEN, Christensen S, Shirley DG. Amiloride inhibits proximal tubular reabsorption in conscious euvolemic rats. *Eur J Pharmacol* 2002; 437: 85–90

Received for publication: 14.9.05
Accepted in revised form: 7.12.05